International Journal Of
Industrial Electronics Control and Optimization
Print ISSN: 3517-2645
Online ISSN: 3568-2645
Homepage: https://ieco.usb.ac.ir/

A min-max approach for energy management of renewable-based electricity-hydrogen microgrids with demand response

Hamid Karimi, and Hamid Reza Sezavar
Department of Electrical and Computer Engineering, Qom University of Technology, Qom, Iran.
Corresponding author's email: Karimi.h@qut.ac.ir

Article Info

Article type:
Research Article

Article history:
Received: **********
Received in revised form: **********
Accepted: **********
Published online: **********

Keywords:
Renewable energy,
Demand response,
Microgrid,
Hydrogen-based microgrid,
Long short-term memory.

ABSTRACT

This paper presents a multi-objective energy management strategy for a hybrid electricity-hydrogen microgrid (MG) aimed at improving economic and operational performance. The proposed framework simultaneously minimizes total operating cost and reduces peak load, which are conflicting objectives in MG operation. To address this challenge, the problem is formulated as a multi-objective optimization model using a normalized weighted sum approach, enabling an effective trade-off between objectives while preventing the creation of new peaks in the load profile. The studied hydrogen-based MGs includes renewable energy sources such as solar and wind power, a battery energy storage system (BESS), a diesel generator, and demand response programs. Hydrogen is also utilized as an energy carrier to enhance system flexibility and support improved integration of renewable generation. Coordinated scheduling of generation units, storage systems, and flexible loads improves system efficiency. To enhance model accuracy, a long short-term memory (LSTM) forecasting method is applied to predict solar irradiance and wind speed using historical data, supporting more reliable scheduling decisions. The proposed model is validated through a general case study. Simulation results show a peak load reduction of 442 kW and an improvement in the load factor of 16.75%, confirming the effectiveness of the proposed approach.

NOMENCLATURE

DR	Demand response	h	Index of hydrogen system
MG	Microgrids	i	Index of non-renewable resources
RES	Renewable energy sources	l	Index of load
SoC	State-of-charge	s	Index of scenarios
b	Index of battery storage system	t	Index of times
c	Index of capacitors		

I. Introduction

Renewable energy sources (RES) such as photovoltaic, wind energy are becoming important as the world seeks sustainable alternatives to fossil fuels [1]. Their environmental benefits, including reduced carbon footprint and lower ecological impact, make them essential components of modern energy strategies. However, the intermittent and variable nature of many RES creates different challenges for stability, reliability, and efficiency of the energy systems [2, 3]. To address these challenges, the concept of microgrids (MGs) has been created as a flexible and resilient solution [4, 5]. A MG is a local energy system that integrates distributed energy resources, energy storage, and controllable loads. The MGs are able to operate as islanded mode or grid-connected mode. By incorporating RES with smart control technologies, MGs enhance energy reliability, support grid stability, and enable efficient energy management at the community, industrial, or campus scale [6, 7]. As a result, MGs are known as key enablers of the transition toward a low carbon energy system [8].

In recent years, different studies are focused on the energy scheduling of MGs. Reference [9] presents a hybrid operation scheduling and peer-to-peer energy trading for MGs to maximize its profit and reduce the electricity unbalance. The proposed model is formulated as mixed integer linear programs, where the deep learning approach has been developed to forecast the loads and RES generation. The authors in [10] proposed a multi-objective optimization

for economic and sustainable operation of MGs. The proposed structure integrates the RES, fuel cell, microturbine, energy storage systems, electric vehicles, and demand response programs (DRP) to investigate the impact of different weather conditions on the MG operation. An advanced dynamic programming approach has been developed in [11] to manage the uncertainty of RES in the energy management of MGs. In this study, the probability distribution functions have been utilized to model the uncertainty of RES. The authors in [12] studied the supply-demand balance in RES-based MG.

Reference [13] studies the optimal sizing of hybrid MG that integrates the RES, AC loads, DC loads, and energy storage systems. The presented model decides to minimize the levelized cost of energy and carbon emission in the scheduling horizon. A two-stage robust scheduling mechanism has been developed in [14] to manage the operation of multi-carrier MG. In the first stage, the optimal sizing of photovoltaic panel, wind turbine, combined heat and power has been defined. The second stage is responsible for determining the optimal operation of electrical and heat systems. Reference [15] proposed a techno-economic model for optimal sizing and optimal operation of AC MG using genetic algorithm. The proposed model investigates the voltage stability and resiliency of MGs in both islanded and grid-connected modes. The particle swarm optimization algorithm has been developed for the AC/DC MG under dynamic tariffs. The proposed model considered the DRP and battery energy storage systems to minimize the total cost of MGs. A Honey Badger Algorithm has been developed in [16] to improve the energy flow in MGs. However

The authors in [17] propose a stochastic approach for peer-to-peer energy trading in the integrated electricity and gas networks. The power-to-gas systems are considered to increase the flexibility of the MGs. However, the peak load reduction is not the main focus of the proposed study. A multi-objective scheduling algorithm is presented in [18] that simultaneously optimizes the operating cost and flexibility of MGs. In this study, the energy storage systems are considered as the main flexible resources in the MGs. Although the proposed model considers the uncertainty of RES, the Long Short-Term Memory (LSTM) is not utilized to predict the RES generation from historical data. Reference [19] considers the economic, environmental, and reliability indices to present a comprehensive scheduling for the MG. To this end, the artificial bee colony and a sine-cosine algorithm are utilized to find the optimal solution for MGs. However, the peak load reduction by the min-max algorithm is not studied.

In this paper, we propose a multi-objective optimization model to simultaneously minimize the total cost and peak load in a hydrogen-based MG. The proposed MG is operated in the grid-connected mode and is integrated with RES, diesel generator, battery storage system, and controllable loads. Also, the MG system utilizes the power-to-hydrogen, hydrogen to power, and hydrogen storage tank to increase the flexibility of MGs and manage the uncertainty of RES. To estimate the production of the RES, the long short-term memory approach has been developed in the proposed model. This approach considers the weather conditions for 365 days to provide more reliable data for RES generation. The main contribution of the work is formulated as follows:

- Proposing a multi-objective model that simultaneously minimizes the total cost and peak load of MGs.
- The proposed model provides a link between electricity and hydrogen in the local energy system. Also, the MG is able to sell the hydrogen to industrial to get more profit.
- Applying the long short-term memory approach to estimate the production of RES and create more reliable results.

The rest of this paper is organized as follows:

Section 2 presents the mathematical formulation of the proposed model. Section 3 describes the numerical results and simulation analysis. Finally, section 4 presents the conclusion and future works.

II. Mathematical formulation of hydrogen-based MG

This section models the objective functions and the equal and unequal constraints of the hydrogen-based MG.

A. Objective functions

The hydrogen-based MG considers both operating cost and peak reduction as objective functions and solves a multi-objective optimization to define the best scheduling. Equations (1) and (2) model the operation cost and peak load reduction, respectively.

$$\min \sum_t \delta_t^E P_t^{Grid} - \sum_t \delta_t^E P_t^{sell} + \sum_i \sum_t (\alpha_i + \beta_i \zeta_i) P_{i,t} + \gamma_i u_{i,t} - \sum_h \sum_t \delta_t^h H_{h,t}^{sell} \quad (1)$$

$$\min \text{Max } P_{l,t}^{DR} \quad (2)$$

The first term of Eq. (1) refers to the cost of imported electricity from the grid. The second term shows the selling electricity to the grid. The third term in Eq. (1) considers the production cost of local resources. The fourth term of Eq. (1) shows the selling hydrogen to industries. According to Eq. (2), a min-max approach is presented to decrease the peak load. The Equation (2) can be replaced by Eq. (3).

$$\begin{aligned} &\min \lambda \\ &\text{S.t:} \\ &\lambda \geq P_{l,t}^{DR} \end{aligned} \quad (3)$$

λ is a free variable that finds the peak load and Eq. (3) tries to reduce λ. Actually, λ is an auxiliary variable that finds the highest demand over the time horizon. By minimizing this variable, the optimization problem effectively reduces the peak load. This approach simplifies the original optimization problem while keeping the reasoning clear and easy to follow.

To solve this multi-objective optimization problem, a normalized approach is used according to Eq. (4) to convert the problem into a single-objective.

$$\min \left\{ \frac{\begin{array}{l}(\sum_t \delta_t^E P_t^{Grid} \\ +\sum_i \sum_t (\alpha_i + \beta_i \zeta_i) P_{i,t} + \gamma_i u_{i,t} \\ -\sum_h \sum_t \delta_t^h H_{h,t}^{sell})\end{array}}{\text{Cost}^*} + \frac{\lambda}{\lambda^*} \right\} \quad (4)$$

S.t:

$\lambda \geq P_{l,t}^{DR}$

Where $Cost^*$ and λ^* are the ideal solutions for cost function and λ, respectively. The normalized weighted sum approach provides different advantages for MGs. This method is able to consider the objective functions with different types and scales. Also, the simplicity of this method is another of its advantages. This method presents a unique solution, and there is no need for solution ranking methods. Due to these advantages, the normalized weighted sum approach is used to handle the proposed multi-objective optimization. However, the main limitation of the proposed model is its sensitivity to the weights of objective functions.

B. Distributed energy resources

Equations (5)-(8) presents formulation of distributed energy resources.

$$u_{i,t} P_i^{\min} \leq P_{i,t} \leq u_{i,t} P_i^{\max} \quad (5)$$

$$P_{i,t} - P_{i,t-1} \leq R_i^{\max,up} \quad (6)$$

$$P_{i,t-1} - P_{i,t} \leq R_i^{\max,down} \quad (7)$$

$$\text{cost}^{DG} = \sum_i \sum_t (\alpha_i + \beta_i \zeta_i) P_{i,t} + \gamma_i u_{i,t} \quad (8)$$

Equation (5) shows the acceptable generation of resources. The ramp-up and ramp-down limits are represented in Eqs. (6) and (7), respectively. Finally, Eq. (8) calculates the production cost of resources.

C. Energy trading with main grid

Equation (9) limits the imported electricity from the main grid. Also, Eq. (10) shows the selling energy with main grid.

$$P^{g,\min} \leq P_t^{Grid} \leq P^{g,\max} \quad (9)$$

$$P^{sell,\min} \leq P_t^{sell} \leq P^{sell,\max} \quad (10)$$

D. Demand response programs

Equations (11)-(13) present the formulation of DR programs. Equation (11) shows the acceptable load shifting level or DR participation level. Equation (12) calculates the shifted load to each time slot. Finally, Eq. (13) presents the new load profile after DR programs.

$$DR^{\min} \leq DR_{l,t} \leq DR^{\max} \quad (11)$$

$$\sum_{t=1}^{T} ldr_{l,t} = \sum_{t=1}^{T} P_{l,t}^{load} DR_{l,t} \quad (12)$$

$$P_{l,t}^{DR} = P_{l,t}^{load} (1 - DR_{l,t}) + ldr_{l,t} \quad (13)$$

E. Battery storage devices

Equations (14)-(19) model the operation constraints of energy storage devices.

$$SoC_{b,t+1} = SoC_{b,t} + \Delta T (\eta_b^{ch} P_{b,t}^{ch} - \frac{P_{b,t}^{disch}}{\eta_b^{disch}}) \quad (14)$$

$$SoC_b^{\min} \leq SoC_{b,t} \leq SoC_b^{\max} \quad (15)$$

$$0 \leq P_{b,t}^{ch} \leq X_{b,t}^{ch} P_b^{ch} \quad (16)$$

$$0 \leq P_{b,t}^{disch} \leq X_{b,t}^{disch} P_b^{disch} \quad (17)$$

$$X_{b,t}^{ch} + X_{b,t}^{disch} \leq 1 \quad (18)$$

$$SoC_{b,t1} = SoC_{b,t4} \quad (19)$$

The stored electricity in the battery is given by Eq. (14). The minimum and maximum stored electricity is determined by Eq. (15). Equations (16) and (17) limit the charging and discharging rates, respectively. Equation (18) prevents from both charging and discharging at each time slot. Finally, Eq. (19) ensures that the initial and final energy in storage system should be equal.

F. Photovoltaic energy

Equation (20) presents the production of photovoltaic panels.

$$P_{i,t}^{PV} = \eta^{PV} N_i^{PV} S_i^{PV} I_t (1 - 0.005 (T_t^{Out} - 25)) \quad (20)$$

G. Wind energy

Equation (21) models the production of wind turbines.

$$P_{i,t}^{WT}=\begin{cases}0 & 0\le v_t\le v_{ci}\ or\ v_{co}\le v_{t,s}\\ P_{i,r}^{WT}\dfrac{v_{t,s}^2-v_{ci}^2}{v_{i,r}^2-v_{ci}^2} & v_{ci}\le v_t\le v_{i,r}\\ P_{i,r}^{WT} & v_{i,r}\le v_t\le v_{co}\end{cases} \quad (21)$$

H. Hydrogen systems

Equations (22)-(29) developed the mathematical formulation of hydrogen storage system, hydrogen-to-electricity, and electricity-to-hydrogen.

$$P_{h,t}^{E\to H_2}\chi_{h,t}=H_{h,t}^{in} \quad (22)$$

$$HL_{h,t}=\begin{cases}HL_{h,t}^0 & t=1\\ HL_{h,t-1}+\left(\phi_{h,t}H_{h,t}^{in}-\dfrac{H_{h,t}^{out}}{\varphi_{h,t}}\right) & t\ge 2\end{cases} \quad (23)$$

$$H_{h,t}^{out}=H_{h,t}^{E}+H_{h,t}^{sell} \quad (24)$$

$$H_{h,t}^{E}\psi_h=P_{h,t}^{H_2\to E} \quad (25)$$

$$HL_h^{\min}\le HL_{h,t}\le HL_h^{\max} \quad (26)$$

$$HL_{h,t}^{E}\le\chi_{h,t}HL_h^{E,\max} \quad (27)$$

$$HL_{h,t}^{sell}\le\sigma_{h,t}HL_h^{sell,\max} \quad (28)$$

$$\sigma_{h,t}+\chi_{h,t}\le 1 \quad (29)$$

Equation (22) shows the amount of generated hydrogen by electrolyzer unit as electricity to hydrogen unit. Equation (23) describes the hourly stored hydrogen in the storage tank. According to Eq. (24), the output hydrogen of hydrogen storage tank can be sold to industries or consumed by fuel cell unit to generate the electricity. Equation (25) calculates the amount of generated electricity by hydrogen-to-electricity unit. Equation (26) limits the minimum and maximum capacity of hydrogen storage tank. Equations (27) and (28) show the maximum bounds of input hydrogen to fuel cell and selling hydrogen to the industries, respectively. Finally, Eq. (29) shows that the hydrogen system sells the generated hydrogen or consumes it by fuel cell units at time *t*.

I. Active and reactive power balances

The active and reactive balance in the hydrogen-based MG is presented in Eqs. (30) and (31), respectively.

$$\begin{aligned}&P_t^{Grid}+\sum_i P_{i,t}+\sum_i(P_{i,t}^{PV}+P_{i,t}^{WT})\\ &+\sum_b(P_{b,t}^{disch}-P_{b,t}^{ch})+\sum_h P_{h,t}^{H_2\to E}=\\ &P_t^{sell}+\sum_h P_{h,t}^{E\to H_2}+\sum_l P_{l,t}^{flex}\end{aligned} \quad (30)$$

$$\begin{aligned}&Q_t^{Grid}+\sum_i(Q_{i,t}+Q_{i,t}^{PV}+Q_{i,t}^{WT})\\ &+\sum_b Q_{b,t}+\sum_c Q_{c,t}=\sum_l Q_{l,t}\end{aligned} \quad (31)$$

III. Simulation Results

A. **Long Short-Term Memory (LSTM) Model for Renewable Generation Forecasting**

To enhance the reliability of the proposed energy management system, a Long Short-Term Memory (LSTM) neural network is employed to forecast the intermittent generation of renewable energy sources (RES), specifically photovoltaic (PV) and wind turbine (WT) outputs. LSTM is a type of recurrent neural network (RNN) well-suited for time-series forecasting due to its ability to capture long-term dependencies and temporal patterns in sequential data. The LSTM model consists of memory cells that regulate the flow of information through three gates: the input gate, forget gate, and output gate. These gates enable the model to retain or discard information over long sequences, mitigating the vanishing gradient problem commonly encountered in traditional RNNs.

Historical data of weather parameters-including solar radiation, ambient temperature, and wind speed-are used as inputs to the LSTM model. The dataset comprises 365 days of hourly records, ensuring seasonal and diurnal variations are captured. The model is trained to predict the next 24-hour generation profile for PV and WT systems. The LSTM model is implemented using the TensorFlow/Keras framework. The dataset is split into training (70%), validation (15%), and testing (15%) sets. The model is trained using the Adam optimizer with mean squared error (MSE) as the loss function. Early stopping and dropout regularization are applied to prevent overfitting.

The performance of the LSTM forecaster is evaluated using the Root Mean Square Error (RMSE) and Mean Absolute Percentage Error (MAPE), according to Eqs. (32) and (33), respectively.

$$RMSE=\sqrt{\frac{1}{N}\sum_{i=1}^{N}(y_i-\hat{y}_i)^2} \quad (32)$$

$$\text{MAPE}=\frac{100\%}{N}\sum_{i=1}^{N}\left|\frac{y_i-\hat{y}_i}{y_i}\right| \quad (33)$$

where y_i is the actual generation and $\hat{y}_i$ is the forecasted value. The internal structure of the Long Short-Term Memory (LSTM) unit used for the renewable energy forecasting model is shown in Fig. 1. The diagram illustrates the information flow through the cell state (*Ct*) and hidden state (*ht*), controlled by the three distinct gating mechanisms: the Forget Gate (discarding irrelevant historical weather data), the Input Gate (updating the cell with new solar/wind features), and the Output Gate.

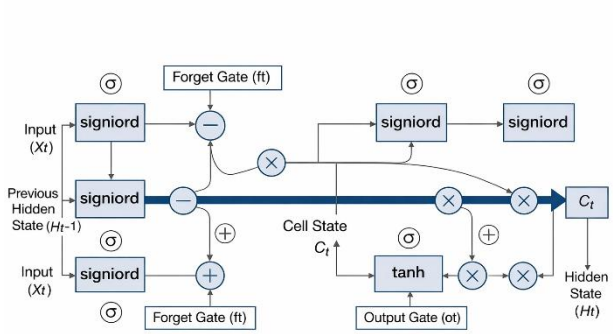

Fig. 1 LSTM model

B. Results

The multi-objective optimization model is tested on 33-bus IEEE test system. Three wind turbines and photovoltaic panels are located in the test system. Table 1 presents the characteristics of wind turbines. Also, three diesel generators are located in bus number 6, 19, and 32 whose characteristics are provided in Table 2. Besides, Fig. 2 and Fig. 3 show the wind speed and solar radiation, respectively.

Table 1 characteristic of wind turbine

	Rated power (kW)	Rated speed (m/s)	Cut-in speed (m/s)	Cut-out speed (m/s)
WT1	225	13.5	3.5	25
WT2	100	13	4.5	25
WT3	90	16.8	3.3	28

Table 2 characteristic of diesel generators

	Capacity (kW)	Min generation (kW)	Ramp-up (kW)	Ramp-down (kW)
DG1	100	10	50	50
DG2	500	100	125	125
DG3	500	100	125	125

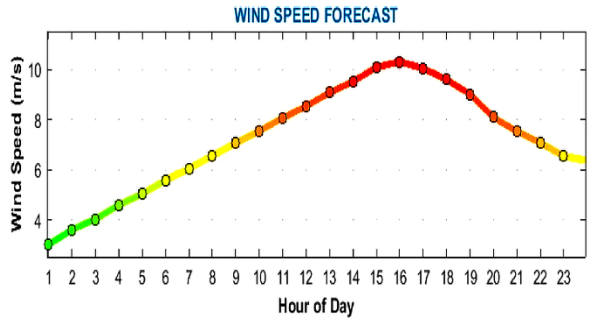

Fig. 2 generated wind speed by LSTM

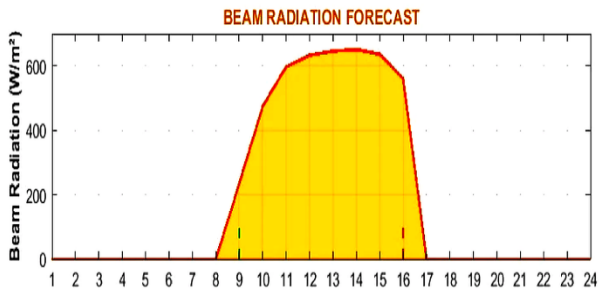

Fig. 3 generated solar radiation by LSTM

The maximum DR participation is considered 20%. The maximum power purchased from the electricity grid is 1200 kW for each time slot. Two hydrogen storage tank is considered with capacities 100 and 150 m^3. The two following case studies are assumed:

- Case study 1: The hydrogen-based MGs only consider the operation cost as an objective function and peak reduction is not considered.
- Case study 2: In this case study, the hydrogen-based MGs considers both operation cost and peak reduction simultaneously.

Table 3 compares the performance of case studies 1 and 2.

Table 3 comparison of case studies 1 and 2

Case study	Operating cost ($)	Peak load (kW)	L.F (%)
Single-objective	6299.18	2637.89	68.03
Multi-objective	6678.65	2195.92	81.72

Table 3 shows that the proposed multi-objective model reduces the peak load by 16.75% because it considers peak reduction as one of its objective functions. Therefore, the MGs perform a coordinated DR program to reduce the peak load. Also, this coordinated DR program increases the load factor and uniformizes the load profile. According to the results, the proposed multi-objective model improves the load factor by 20.12 %. This improvement is provided because the coordinated DR programs decrease the peak load and fill the valley load. Finally, Fig. 4 shows the load profile of the hydrogen-based MGs in both case studies.

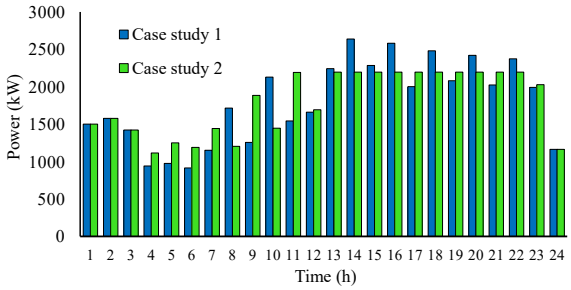

Fig. 4 load profile in case studies 1 and 2

The results of Fig. 4 indicate that the proposed model significantly decreases the peak load of the hydrogen-based MGs compared to case study 1. Actually, MGs reduce their energy consumption during peak hours and shift it to the off-peak hours. This performance reduces the operating cost of hydrogen-based MGs because electricity tariffs during off-peak hours are lower than those during peak hours. Fig. 5 presents the DR participation level for different loads.

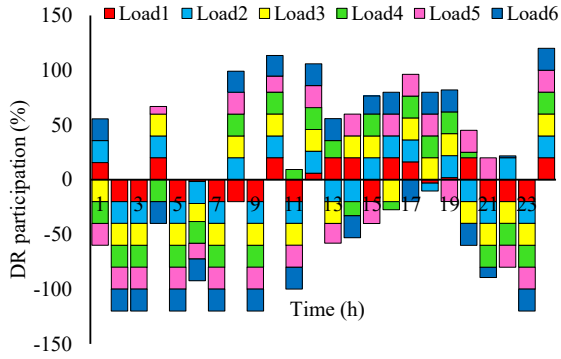

Fig. 5 DR participation level in the proposed model

The positive and negative values show the downward and upward DR, respectively. The results show that during peak hours, the hydrogen-based MGs reduce their energy consumption. Two reasons exist for this performance. First, the difference between off-peak and peak hours encourages the hydrogen-based MGs to shift their loads. Second, the proposed model attempts to reduce the peak load using a min-max approach. Fig. 6 presents the purchased electricity from the main grid.

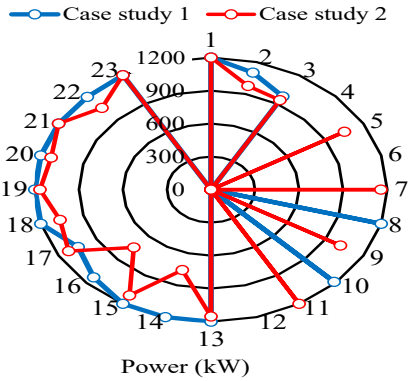

Fig. 6 purchased electricity from the main grid

The results of Fig. 6 show that at the beginning of the day, the hydrogen-based MGs import less energy from the main grid because its loads are lower and its distributed energy sources can supply the needed energy. However, during peak hours, the hydrogen-based MGs increase the imported energy from the electricity network to meet the required loads.

Figures 7 and 8 show a complete comparison of the three forecasting methods. In Figure 7, the solar energy production forecasts are displayed alongside the actual measured values. In this section, the base model, or Persistent, has the weakest results, as it is associated with a delay and cannot accurately represent the correct time and peak of daily production. This result is not unexpected, since the model assumes that the next value is exactly equal to the last value and therefore cannot predict the daily cycle of the sun. The ARIMA model performs better than the base model and detects the overall daily trend. However, it still has significant errors during peak production hours and times when production decreases or increases. The reason for this limitation is that the ARIMA model is based on linear relationships and cannot model well the nonlinear variations in solar radiation that occur due to factors such as clouds and atmospheric conditions. However, the LSTM model we have proposed performs much better and tracks the actual production, which is marked with a black line, with high accuracy over the entire 48-hour period. In Figure 8, the forecasts for wind turbine production are compared. Wind energy forecasting has its own difficulties because wind energy is highly variable, has little stability, and depends on various atmospheric factors. The baseline model also performs poorly here because the wind speed is constantly changing, violating the assumption of the baseline model being stationary. The ARIMA model has been able to improve the performance to some extent and detect some of the dependencies in the wind data. However, it is unable to predict sudden changes and accurately record the peaks.

In Figure 9, a numerical evaluation using the RMSE criterion is performed for all three methods and both solar and wind turbines. For PV forecasting, the Persistent model achieves an RMSE of 85.2 kW, which serves as the baseline. The ARIMA model reduces this to 39.1 kW, representing a 54.1% improvement by capturing basic diurnal patterns. The proposed LSTM model further reduces RMSE to 22.9 kW, achieving a 41.6% improvement over ARIMA and a 73.1% total reduction from the Persistent baseline. This progressive improvement demonstrates that while ARIMA captures fundamental patterns, LSTM's deep learning architecture achieves substantially higher accuracy by modeling the nonlinear relationships in solar generation data. For wind forecasting, the Persistent model shows an RMSE of 78.5 kW. ARIMA improves this to 59.2 kW (24.6% reduction), capturing some autocorrelation structure. LSTM achieves an RMSE of 40.3 kW, representing a 31.9% improvement over ARIMA and a 48.7% total reduction from Persistent. The higher absolute RMSE values for wind compared to PV across all methods reflect the inherently greater stochastic nature of wind resources. However, LSTM still achieves substantial improvement, demonstrating its effectiveness even for highly variable processes.

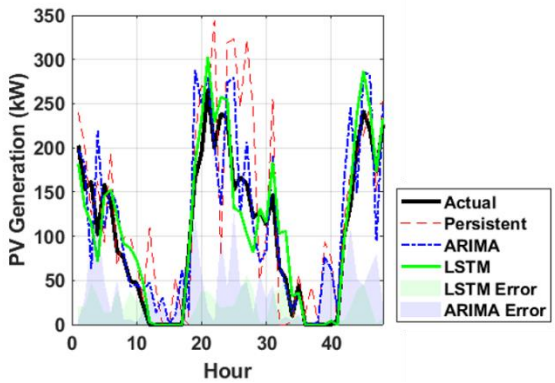

Fig. 7 Comparison of solar power forecasts with actual values using Persistent, ARIMA, and LSTM models.

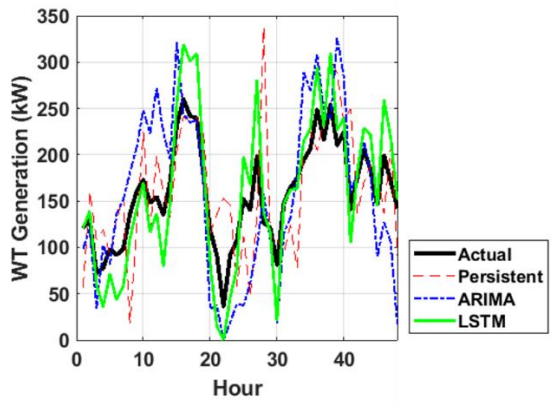

Fig. 8 Comparison of wind power forecasts with actual values using Persistent, ARIMA, and LSTM models.

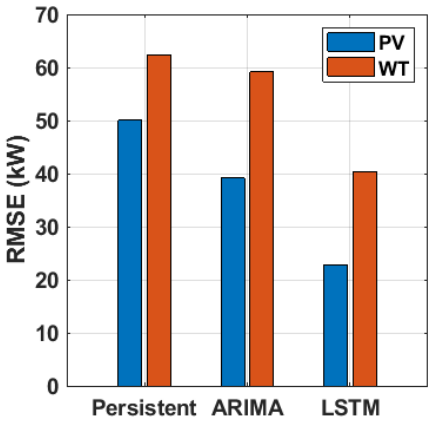

Fig. 9 RMSE-based performance comparison of Persistent, ARIMA, and LSTM models for solar and wind forecasting.

Table 4 presents the impact of DR participation level on the operating cost and peak load of hydrogen-based MGs.

Table. 4 sensitivity analysis on DR participation level

DR participation (%)	Cost ($)	Peak load (kW)
0	8559.55	2590
10	7357.55	2331.03
15	7066.90	2204.4
20	6678.65	2195.92

The numerical results show that by increasing DR participation level from 0 % to 20 %, the operating cost of hydrogen-based MGs is decreased by 21.97 %. The main reason for the cost reduction in hydrogen-based MGs is that the higher DR participation level increases their ability to shift the energy consumption from peak hours to off-peak. This load shifting also decreases the peak load by 15.21 % and helps the hydrogen-based to flatten their load profiles. Table 5 shows the impact of electricity prices on the performance of the proposed model. Accordingly, electricity prices are scaled from 0.5 to two times the base-case values, and the results are reported in Table 5.

Table 5 impact of electricity prices on the performance of hydrogen-based MGs

Price coefficient	Cost ($)	Peak load (kW)
0.5	3047.74	2072.02
1	6678.65	2195.92
1.5	9740.43	2246.16
2	12679.54	2246.16

The numerical results present that increasing the electricity prices increases the operating cost of the hydrogen-based MGs because the hydrogen-based MGs must pay a higher cost for purchasing energy from the main grid. The numerical results show that when the electricity prices are doubled, the operating cost of hydrogen-based MGs is increased by 89.85 %.

To evaluate the computational complexity and scalability of the proposed multi-objective model, the number of hydrogen-based MGs is increased from 3 to 6, 9, and 12. The results for different conditions are indicated in Table 6.

Table 6 computational scalability of the proposed model

No. of MGs	No. of single constraints	No. of single variables	No. of discrete variables
3	3,952	1,808	360
6	5,110	2,603	576
9	6,487	3,542	792
12	7,864	4,481	1,008

The results show that by increasing the number of hydrogen-based MGs, the proposed model remains computationally tractable. When the number of the hydrogen-based MGs is 12, the execution time reaches 128 seconds. This execution time is acceptable for practical applications because the proposed model is intended for day-ahead energy scheduling.

IV. Conclusions

This paper presents a multi-objective optimization framework that simultaneously minimizes the total cost and peak load of hydrogen-based MGs in the distribution network. In the proposed structure, the hydrogen-based MGs integrate renewable generation, battery energy storage, demand response programs, and a hydrogen system to increase the system's flexibility. To control the uncertainty of renewable generation, the long short-term memory approach is used to predict the generation of photovoltaic and wind energy. In the proposed model, the demand response programs provide the opportunity for cost savings for hydrogen-based MGs by load shifting during peak hours to off-peak hours. The numerical results show that the DR programs reduce the peak load by 15.21 %. Additionally, the proposed model increases the load factor of hydrogen-based MGs by 16.75 % through controllable DR programs. In future works, a multi-layer framework will be proposed to simultaneously consider both economic and power quality indices in the operation scheduling of hydrogen-based MGs.

Funding

This work is based upon research funded by Iran National Science Foundation (INSF) under project No 4040919.

References

[1] Opoku, Eric Evans Osei, Alex O. Acheampong, Kingsley E. Dogah, and Isaac Koomson. "Energy innovation investment and renewable energy in OECD countries." *Energy Strategy*

Reviews, vol. 54, 2024, 101462, DOI: 10.1016/j.esr.2024.101462.
[2] Bassey, Kelvin Edem, Ayanwunmi Rebecca Juliet, and Akindipe O. Stephen. "AI-Enhanced lifecycle assessment of renewable energy systems." *Engineering Science & Technology Journal*, vol. 5, no. 7, 2024, pp. 2082-2099, DOI: 10.51594/estj/v5i7.1254.
[3] Bennagi, Aseel, Obaida AlHousrya, Daniel T. Cotfas, and Petru A. Cotfas. "Comprehensive study of the artificial intelligence applied in renewable energy." *Energy Strategy Reviews*, vol. 54, 2024, 101446, DOI. 10.1016/j.esr.2024.101446.
[4] Chen, Lei, Lingyun Gao, Shuping Xing, Zhicong Chen, and Weiwei Wang. "Zero-carbon microgrid: Real-world cases, trends, challenges, and future research prospects." *Renewable and Sustainable Energy Reviews*, vol. 203, 2024, 114720, DOI: 10.1016/j.rser.2024.114720.
[5] Arévalo, Paul, Dario Benavides, Danny Ochoa-Correa, Alberto Ríos, David Torres, and Carlos W. Villanueva-Machado. "Smart microgrid management and optimization: a systematic review towards the proposal of smart management models." *Algorithms*, vol. 18, no. 7, 2025, 429, DOI: 10.3390/a18070429.
[6] Punitha, S., N. P. Subramaniam, and P. Ajay D. Vimal Raj. "A comprehensive review of microgrid challenges in architectures, mitigation approaches, and future directions." *Journal of Electrical Systems and Information Technology*, vol. 11, no. 1, 2024, DOI: 10.1186/s43067-024-00188-4.
[7] Juma, Shaibu Ali, Sarah Paul Ayeng'o, and Cuthbert ZM Kimambo. "A review of control strategies for optimized microgrid operations." *IET Renewable Power Generation*, vol. 18, no. 14, 2024, pp. 2785-2818, DOI: 10.1049/rpg2.13056.
[8] Zhao, Bingxu, Xiaodong Cao, and Pengfei Duan. "Cooperative operation of multiple low-carbon microgrids: An optimization study addressing gaming fraud and multiple uncertainties." *Energy*, vol. 297, 2024, 131257, DOI: 10.1016/j.energy.2024.131257.
[9] Ravivarma, K., B. Lokeshgupta, and Ramanjaneya Reddy Udumula. "A blockchain based peer-to-peer energy trading model for multi microgrid distributed energy management." *Sustainable Energy, Grids and Networks*, vol. 44, 2025, 102045, DOI: 10.1016/j.segan.2025.102045.
[10] Wen, J., Sergey Zhiltsov, Rustem Shichiyakh, Samariddin Makhmudov, Muzaffar Shojonov, Anorgul I. Ashirova, and M. Mohammadi. "Economic and environmental multi-objective functions modeling in storage systems-based hybrid energy microgrid with demand side management strategy." *Sustainable Computing: Informatics and Systems*, vol. 48, 2025, 101245, DOI: 10.1016/j.suscom.2025.101245.
[11] Shaterabadi, Mohammad, Mehdi Ahmadi Jirdehi, Vahid Sohrabi Tabar, and Sadjad Galvani. "Advanced dynamic programming for optimal microgrid energy management under RER intermittency." *Renewable Energy*, vol. 256, 2025, 124077, DOI: 10.1016/j.renene.2025.124077.
[12] Zhang, Liping, Chenrui Qu, Qingcheng Zeng, and Junying Song. "Optimal energy management for wind-powered port microgrids considering energy supply-demand matching strategy." *Ocean Engineering*, vol. 343, 2026, 123186, DOI: 10.1016/j.oceaneng.2025.123186.
[13] Alilou, Masoud, Abdollah Younesi, and Pierluigi Siano. "A sustainable approach to hybrid microgrid design: Optimal sizing and energy management." *Renewable Energy*, vol. 256, 2026, 124078, DOI: 10.1016/j.renene.2025.124078.
[14] Mojtaba Hadi, Elhoussin Elbouchikhi, Zhibin Zhou, Abdelhakim Saim, "Robust Optimization for Multi-Energy Microgrid Sizing and Energy Management under Load Uncertainty with Demand Response", *Results in Engineering*, 2025, 108609, DOI: 10.1016/j.rineng.2025.108609.
[15] Chrif, Ayoub, Elhoussin Elbouchikhi, Abdelmajid Abouloifa, and Mohamed Machmoum. "Techno-economic sizing and multi-objective energy management of AC multi-bus microgrids for enhanced reliability and cost efficiency: Application to small villages in Morocco." *Energy Conversion and Management: X*, vol. 28, 2025, 101246, DOI: 10.1016/j.ecmx.2025.101246.
[16] Akarne, Youssef, Ahmed Essadki, Maha Annoukoubi, Ssadik Charadi, and Houssam Eddine Chakir. "Enhanced Energy Management System for Smart Microgrids Using an Improved Honey Badger Algorithm." Results in Engineering, vol. 28, 2025, 107244, DOI: 10.1016/j.rineng.2025.107244.
[17] Feili, Meysam, and Mohammad Taghi Aameli. "The P2P energy management scheme for integrated energy microgrid considering P2G and electricity network fee." *International Journal of Industrial Electronics Control and Optimization*, vol. 8, no. 1, 2025, pp. 1-23.
[18] Gholipour Zarandi, Faezeh, Masoud Rashidinejad, Amir Abdollahi, and Ali Yazhari Kermani. "Assessment of Economic, Technical, Social, and Environmental Impact of Flexibility-based Smart Microgrid Operation." *International Journal of Industrial Electronics Control and Optimization*, vol. 8, no. 1, 2025, pp. 57-66.
[19] Shirmardi, Seyed Arman, Mahmood Joorabian, and Hassan Barati. "Green Micro-Grid Operation Constrained to Reliability and Flexibility Indices in the Presence of Distributed Generations and Energy Storage Systems." *International Journal of Industrial Electronics Control and Optimization,* vol. 4, no. 4, 2021, pp. 397-407.

Appendix A

Parameters	
C_{co2}^{Grid} / C_{co2}^{DG}	Emission coefficient of main grid and non-renewable resources
$C_{co2}^{H_2 \to E}$	Emission coefficient hydrogen-to-power units
$DR^{\min}$ / $DR^{\max}$	Min/max DR level
$HL_h^{\min}$ / $HL_h^{\max}$	Min/max level of hydrogen storage
$HL_h^{E,\max}$	Max hydrogen for electricity generation
$HL_h^{sell,\max}$	Max selling hydrogen to industries
I_t / T_t^{Out}	Solar radiation and ambient temperature
P_b^{ch} / P_b^{disch}	Charging/discharging of battery devices
$P^{g,\min}$ / $P^{g,\max}$	Min/max limits of imported energy from grid
$P^{sell,\min}$ / $P^{sell,\max}$	Min/max limits of selling energy to grid
$P_{l,t}^{load}$	Load profile before DR
$P_i^{\min}$ / $P_i^{\max}$	Min/max capacity of non-renewable resources
$P_{i,r}^{WT}$ / $v_{i,r}$	Rated power and rated speed of WT

$Q_{l,t}$	Reactive power of loads
$R_i^{\max,up}$	Ramp-up of non-renewable resources
$R_i^{\max,down}$	Ramp-down of non-renewable resources
$SoC_b^{\min}$ / $SoC_b^{\max}$	Min/max SoC of battery devices
v_{ci} / v_{co}	Cut-in and cut-out speeds of WT
$v_{t,s}$	Wind speed at time t
δ_t^E	Trading electricity prices
α_i	Coefficient cost of non-renewable resources
β_i	Coefficient cost of non-renewable resources
ζ_i	Produced emission of non-renewable resources
γ_i	Fix cost of non-renewable resources
δ_t^h	Trading hydrogen prices
ψ_h	Hydrogen-to-power constant coefficient
$\phi_{h,t}$ / $\varphi_{h,t}$	Charging/discharging efficiency of hydrogen storage
η^{PV} / N_i^{PV} / S_i^{PV}	Efficiency, number, and area of PVs
η_b^{ch} / η_b^{disch}	Charging/discharging of battery devices
Variables	
$\cos t^{DG}$	Generation cost of non-renewable resources
$DR_{l,t}$	DR level of loads
$H_{h,t}^{sell}$	Selling hydrogen to industries
$H_{h,t}^{in}$	Input hydrogen into hydrogen storage
$H_{h,t}^{out}$	Output hydrogen from hydrogen storage
$HL_{h,t}$	Stored hydrogen in storage tank
$H_{h,t}^{E}$	Used hydrogen to produce electricity
$ldr_{l,t}$	Shifted load
$P_{i,t}^{PV}$	Generating power of PVs
$P_{i,t}^{WT}$	Generating power of WTs
P_t^{Grid} / P_t^{sell}	Imported/selling power from/to grid
$P_{i,t}$	Generation of non-renewable resources
$P_{h,t}^{H_2 \to E}$	Generated power by hydrogen-to-power units
$P_{l,t}^{DR}$	Load consumption after load-shifting
$P_{b,t}^{ch}$	Charging power of battery devices
$P_{b,t}^{disch}$	Discharging power of battery devices
$P_{h,t}^{E \to H_2}$	Generated hydrogen by power -to- hydrogen units
Q_t^{Grid}	Reactive power of grid
$Q_{i,t}$	Reactive power of non-renewable resources
$Q_{i,t}^{PV}$	Reactive power of PVs
$Q_{i,t}^{WT}$	Reactive power of PVs
$Q_{b,t}$	Reactive power of battery devices
$Q_{c,t}$	Reactive power of capacitors
$SoC_{b,t}$	SoC of battery devices
$X_{b,t}^{disch}$	Binary variables for discharging of BSS
$X_{b,t}^{ch}$	Binary variables for charging of BSS
$u_{i,t}$	Binary variable of non-renewable resources
$\sigma_{h,t}$	Binary variable for selling hydrogen
$\chi_{h,t}$	Binary variables for injecting output power into hydrogen-to-power

Biography

Hamid Karimi received his B.Sc. and M.Sc. degrees in Electrical Engineering from Shahid Beheshti University (SBU) and Iran University of Science and Technology (IUST), Tehran, Iran, in 2015 and 2017, respectively. He obtained his Ph.D. in Electrical Engineering from Iran University of Science and Technology (IUST) in 2022. His research interests include power system operation optimization, multi-objective optimization, and game theory. He is currently an Assistant Professor at the Faculty of Electrical and Computer Engineering, Qom University of Technology (QUT), Iran.

Hamid Reza Sezavar was born in Qom, Iran, in 1991. He received a B.Sc. degree from the Sharif University of Technology, Tehran, Iran, in 2013 and a M.Sc. in electrical engineering from the University of Tehran, Tehran, Iran, in 2015. He then received his PhD in High Voltage from the University of Tehran, Tehran, Iran, in 2022. He is currently working toward an assistant professor position at Qom University of Technology. His principal research interests are High voltage engineering, outdoor insulators, Electrical discharge, and AI optimization.